Geophysical Research Letters

RESEARCH LETTER
10.1029/2019GL083437

Key Points:
- A hole in the subducting Juan de Fuca slab may be caused by a weak zone in the plate, inherited from formation at the ridge
- The fragmentation of the plate at depth is causing volcanism in North America and deformation in the oceanic plate offshore
- The capture of oceanic plate fragments, and thus the death of oceanic plates, appears to be a bottom-up process

Supporting Information:
- Supporting Information S1

Correspondence to:
W. B. Hawley,
whawley@seismo.berkeley.edu

Citation:
Hawley, W. B., & Allen, R. M. (2019). The fragmented death of the Farallon plate. *Geophysical Research Letters*, *46*, 7386–7394. https://doi.org/10.1029/2019GL083437

Received 23 APR 2019
Accepted 30 JUN 2019
Accepted article online 3 JUL 2019
Published online 11 JUL 2019

The Fragmented Death of the Farallon Plate

William B. Hawley[1,2] and Richard M. Allen[1,2]

[1]Department of Earth and Planetary Science, University of California, Berkeley, CA, USA, [2]Berkeley Seismology Lab, University of California, Berkeley, CA, USA

Abstract The processes that accompany the death of an oceanic plate, as a ridge nears a trench, remain enigmatic. How the plate might reorganize, fragment, and eventually be captured by one of the bounding plates are among the unresolved details. We present a tomographic model of the Pacific Northwest from onshore and offshore seismic data that reveals a hole in the subducted Juan de Fuca plate. We suggest that this hole is the result of a tear along a preexisting zone of weakness, is causing volcanism on the North American plate, and is causing deformation in the Juan de Fuca plate offshore. We propose that in the final stages of an oceanic plate's life, deformation on the surface can be driven by deeper dynamics and that the fragmentation and the eventual capture of oceanic plate fragments may be governed by a process that operates from the bottom up.

Plain Language Summary A hole in a subducted plate, in the mantle beneath North America, may cause volcanism and earthquakes on the surface of the Earth. Volcanism on the surface of North America appears to have been spatially coincident with a known zone of weakness on the slab for the last ~17 million years. We suggest that this hole is caused by tearing along the zone of weakness, a feature that is created when the plate is formed at the ridge. The tearing not only causes volcanism on North America but also causes deformation of the not-yet-subducted sections of the oceanic plate offshore. This tearing may eventually cause the plate to fragment, and what is left of the small pieces of the plate will attach to other plates nearby.

1. Introduction

In principle, the natural end of an oceanic plate's life is when the ridge that creates that plate reaches a subduction zone. Exactly how this occurs in practice, and what geophysical phenomena might accompany it, remains poorly understood. The Cascadia Subduction Zone, where the young Juan de Fuca (JdF) plate subducts beneath the western margin of North America, provides an ideal location to study this process. The JdF plate is the northern remnant of the Farallon plate and represents the final stages of tens of millions of years of continuous subduction beneath the western margin of North America (Atwater, 1970). Furthermore, unsubducted fragments of the Farallon plate remain off the coast of western North America (Atwater, 1970; Wang et al., 2013), having been incorporated into the Pacific plate. These fragments provide a different snapshot in time of the same system, and evidence for how the final state of the Pacific-North America-JdF system might look. In this study, we present an S wave velocity model using seismic data from arrays both onshore and offshore in this region to illuminate the link between subduction zone architecture, subduction dynamics, deformation, and volcanism, both in the subducting and the overriding plates, to shed light on the mechanisms that accompany the death of an oceanic plate.

Two key features that we will address are the internal deformation of the Gorda section of the JdF plate and the High Lava Plains (HLP) volcanic province (Figure 1). The Gorda region, which is the southernmost section of the JdF plate, is undergoing intense deformation, primarily in the form of strike-slip faults that trend NE-SW near the ridge, transitioning to NW-SE farther from the ridge (Wilson, 1989, 2002). This deformation is thought to be because the Mendocino Transform, which bounds the Gorda region to the south, has not reoriented as the Gorda and JdF ridges have rotated clockwise since 10 Ma. The Pacific plate just south of the transform was created at approximately 30 Ma (Atwater, 1970) and is thus colder and stronger than the much younger Gorda region, whose oldest unsubducted fabric was created at only 6 Ma (Wilson, 2002). Furthermore, the rotation of the ridge system has generated propagator wakes (Hey, 1977; Wilson, 1990), which are formed by overlapping segments of the ridge that migrate along the ridge axis. Propagator wakes extend down into the lithospheric mantle and are locally more highly fractured—and likely weaker—than

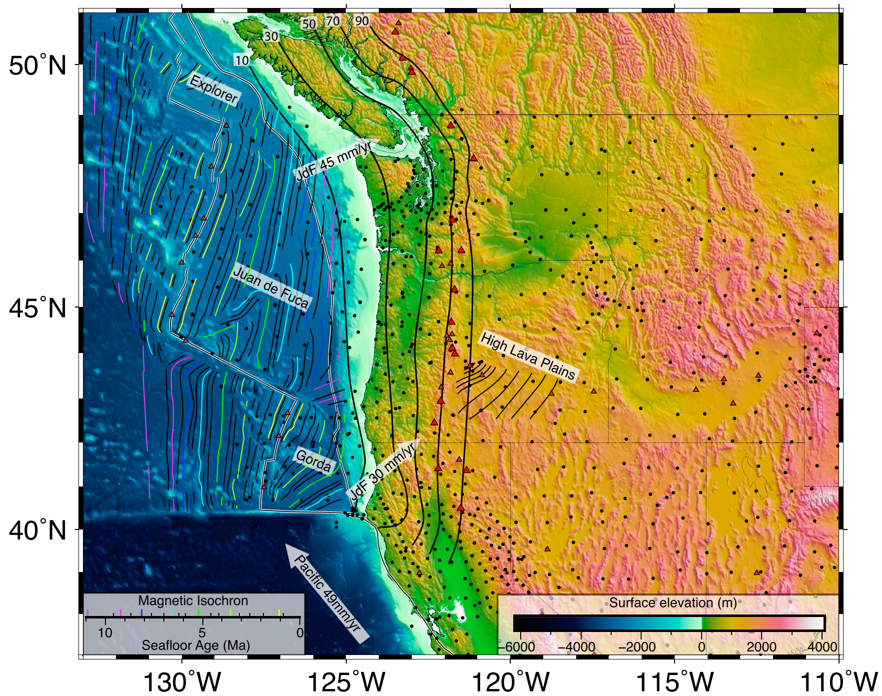

Figure 1. Regional tectonic map with seismic stations used in this study marked as dots. Double white lines indicate plate boundaries; plate motions of the Juan de Fuca and Pacific plates are shown as white arrows relative to North America. Magnetic isochrons offshore are from Wilson (2002). Thick contours east of the subduction zone indicate depth to the Juan de Fuca slab in km (McCrory et al., 2012). Thinner contours in southern Oregon represent 1-Ma isochrons of westward propagating High Lava Plains volcanism (Jordan, 2005).

the rest of the plate (Han et al., 2016; Horning et al., 2016; Nedimović et al., 2009). These features can be seen as offsets in the magnetic anomalies (Figure 1). Propagator wakes have been linked to increased intermediate-depth seismicity due to dehydration (Nedimović et al., 2009).

The HLP is a volcanic province that extends from southeastern to central Oregon. Bimodal volcanism has occurred in the HLP since the mid-Miocene, marked in particular with rhyolitic features that show a distinct age progression, starting in southeastern Oregon, and migrating toward W15°N, at a rate of 33 mm/year from 10 to 5 Ma, and 13 mm/year from 5 Ma to the present (Jordan, 2005). This age progression makes the HLP unique from the other significant volcanism that has occurred in the region in Tertiary time and thus implies a different mechanism. Current volcanism lies approximately 40 km east of the central Cascade arc axis. The age-progressive rhyolitic volcanism, accompanied by widespread basaltic volcanism, resembles in many ways the Yellowstone Snake River Plain, generally considered to be the result of a mantle plume (Camp & Ross, 2004; Pierce & Morgan, 1992). Furthermore, the origin of the age progression for these two provinces appear to be very similar in time and space: the Columbia River Basalt eruptions, at ~17 Ma. While the mantle plume model fits many observations of the Yellowstone volcanic track, it is not consistent with other observations in the HLP, including the direction of age progression (Ford et al., 2013; Jordan, 2005) and helium isotope analysis (Graham et al., 2009). The most complete explanations for the HLP involve the JdF slab, either by a lateral tear in the slab at depth (Liu & Stegman, 2012), by large-scale Farallon-induced mantle flow (Zhou et al., 2018), or by asthenospheric flow induced and focused by rollback of the strong, coherent JdF slab in the upper mantle (Ford et al., 2013; Long et al., 2012).

We generate a tomographic model from teleseismic *S* wave data that shows that the slab below ~150-km depth is discontinuous along strike, consistent with other models of the region (Bodmer et al., 2018; Hawley et al., 2016; James et al., 2011; Obrebski et al., 2010; Roth et al., 2008; Schmandt & Humphreys, 2010). We argue that the discontinuous slab may be driving volcanism in the HLP, similar to results of geodynamic simulations of the region (Liu & Stegman, 2012; Zhou, Liu, & Hu, 2018). We further contend that the fragmentation of the JdF slab at depth is driving deformation on the surface and that the final

10.1029/2019GL083437

stages of the life of an oceanic plate are dominated by bottom-up disintegration, rather than a simple cessation of subduction when the ridge meets the trench.

2. Data and Methods

We construct large-scale 3-D images of the interior structure of the Earth using observations of seismic phases generated by distant earthquakes. Two seismic arrays, the Cascadia Initiative (Toomey et al., 2014) and EarthScope's Transportable Array, provide excellent coverage of the Cascadia Subduction Zone (Figure 1). Using observations of 34,670 direct teleseismic *S* wave arrivals from 217 events on these two arrays and other regional arrays, we have constructed an *S* wave isotropic velocity model of the regional mantle through finite-frequency tomographic inversion. The methodology is detailed in Obrebski et al. (2010). Our model domain is a spherical cap that extends from 27°N to 50°N, from 133°W to 101°W, and from the surface to 2,500-km depth, with 65 nodes in each dimension. The model box is larger than the region in which we expect to have good resolution; delays that are not easily accounted for within the model domain will be absorbed at the edges of the model.

Horizontal components of ocean bottom seismometers are plagued both with uncertainty in orientation and with higher noise, so we have picked the arrivals on the vertical component. The noise characteristics of the ocean bottom seismometers also require that we filter in a narrower band pass (20–40 s) than is commonly performed for onshore body wave tomographic studies. We calculate the frequency-dependent sensitivity kernels (Dahlen et al., 2000). Our inversion minimizes the misfit in delay times by solving simultaneously for the isotropic velocity perturbation at each node, and a single correction term for each station and each event (Figure S1 in the Supporting Information). The station corrections remove delays associated with the sediments and crust immediately beneath the station, minimizing contamination of the mantle velocity structure. Although station correction terms can absorb some of the real signal from the mantle, we choose to incorporate them because imposing crustal and lithospheric velocities introduces uncertainties that are difficult to quantify.

3. Tomographic Model

Our model, CASC19-S, is broadly consistent with CASC16-P, our previous *P* wave model of the region (Hawley et al., 2016), as well as other tomographic models of the Pacific Northwest (Bodmer et al., 2018; James et al., 2011; Obrebski et al., 2010; Roth et al., 2008; Schmandt & Humphreys, 2010). The JdF slab appears as a high seismic velocity feature that trends north and dips to the east (Figure 2). At 80-km depth, this feature is continuous from about 40°N to the edge of our model at 50°N. By 150-km depth, the high-velocity slab is not visible from roughly 44°N to 46°N. While the precise depth of this gap differs from model to model, it is a robust feature of virtually every tomographic model that has been produced in this region, with resolution beneath ~150-km depth, since the deployment of the Transportable Array here in 2006. Most of the models that do have resolution at this depth are teleseismic body wave tomographic models, which generally have lateral resolution on the order of the station spacing, in this case ~70 km. The vertical resolution of this type of model is not as good. Since the rays are traveling nearly vertically in the upper mantle, velocity anomalies tend to be smeared vertically, along the path of the incoming rays. Thus, again, while the depth of the hole is different in the models we reference here, the fact that there is a gap in the high velocities is robust.

The hole has been noted and interpreted by previous authors. Initially, it was proposed to be an artifact owing to significantly reduced velocities in the mantle wedge (Roth et al., 2008). Since then, there has generally been consensus that the hole is not an artifact, but the creation of the hole has been attributed to a range of processes, including Yellowstone plume-induced slab destruction (Obrebski et al., 2010), along-strike variations in dynamic pressure from the mantle beneath the slab (Liu & Stegman, 2011), and simply evidence for complex subduction (James et al., 2011; Schmandt & Humphreys, 2010).

To reiterate that the apparent hole is not an artifact due to low velocities in the overlying mantle wedge, we point to a recent receiver function study (Cheng et al., 2017) that was able to resolve impedance structure between 100 and 200 km, where the hole appears in the tomographic models. A strong high-velocity feature situated immediately beneath a strong low-velocity feature would be difficult to resolve using teleseismic body wave tomography. Because, however, receiver functions are sensitive to sharp vertical velocity

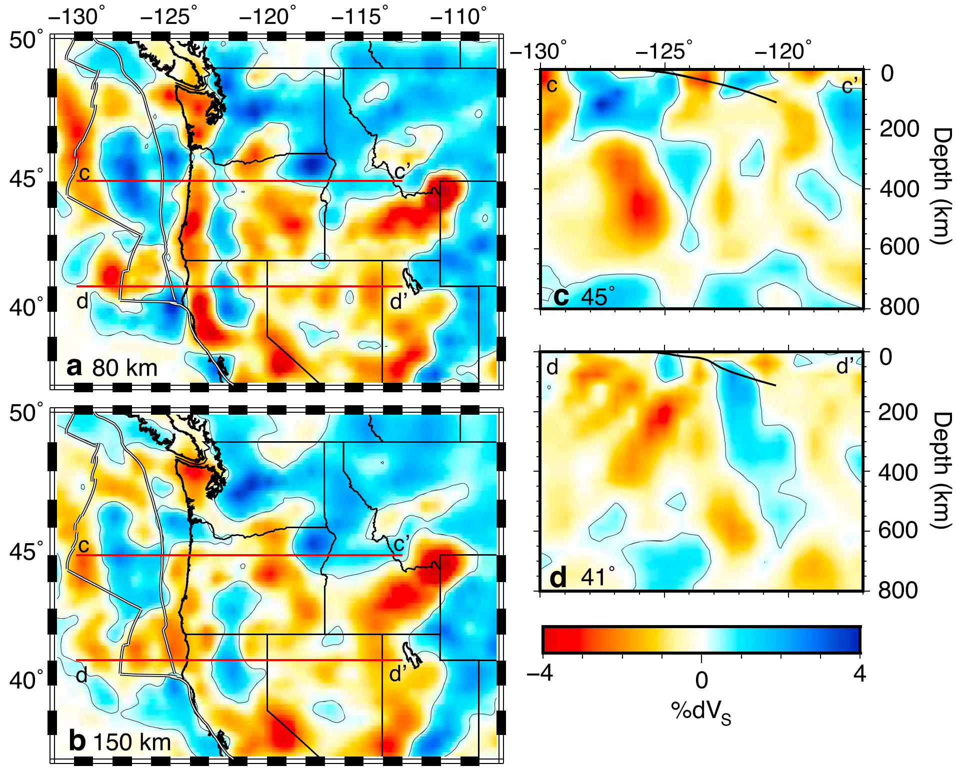

Figure 2. Slices through the tomography model, CASC19-S. Contours represent +0.25% dV_S. In the slice at 80-km depth (a), the slab is continuous north-south, with variations along strike in the strength of the recovered signal. By 150-km depth (b), the slab has a prominent gap between ~44°N and 46°N. The depth extent of the slab is shown in two vertical slices, with a bold slab contour from (McCrory et al., 2012). The slice through the hole at 45°N (c) shows no high-velocity slab feature coincident with the McCrory et al. (2012) slab surface. The other shows that the Gorda slab at 41°N (d) extends at least to 400 km, and possibly 600-km depth.

gradients, such a scenario would be detectable using that method. The fact that the size and depth extent of the hole is similar in both tomographic images and receiver function images makes an artifact an unlikely explanation for the feature.

4. Interpretation

The active expression of the HLP trend lies directly above the southern edge of the slab hole we image in CASC19-S. Slab holes have been inferred in other subduction zones (Obayashi et al., 2009; Portner et al., 2017), sometimes accompanied by anomalous volcanism (Berk Biryol et al., 2011; Rosenbaum et al., 2008). Dry basalts in the HLP have been explained by upwelling mantle in the backarc due to rollback of the coherent JdF slab (Ford et al., 2013; Long et al., 2012; Till et al., 2013), but as the tomography models do not show a coherent slab, we explore the possibility that the volcanism is generated by asthenospheric flow through the hole and subsequent decompression melting.

4.1. Causes of the Hole

The distinct age progression in the HLP suggests that if the volcanism is due to a tear in the slab, that tear is propagating updip. We can then estimate the speed and direction of this tear on the JdF slab by subtracting the JdF motion from the HLP motion, both of which are known with respect to North America (vector sum in Figure 3a). The JdF plate is subducting at ~35 mm/year toward N55°E relative to North America (Wilson, 1993), indicating that the tear velocity in the JdF plate has been, on average, approximately 50 mm/year toward S75°W. This trend closely matches that of a prominent propagator wake in the northern Gorda region (Wilson, 2002; Figure 3a). Since propagator wakes are thought to be weaker than the rest of the plate (Canales et al., 2017; Horning et al., 2016; Nedimović et al., 2009), a tear along this preexisting zone of

10.1029/2019GL083437

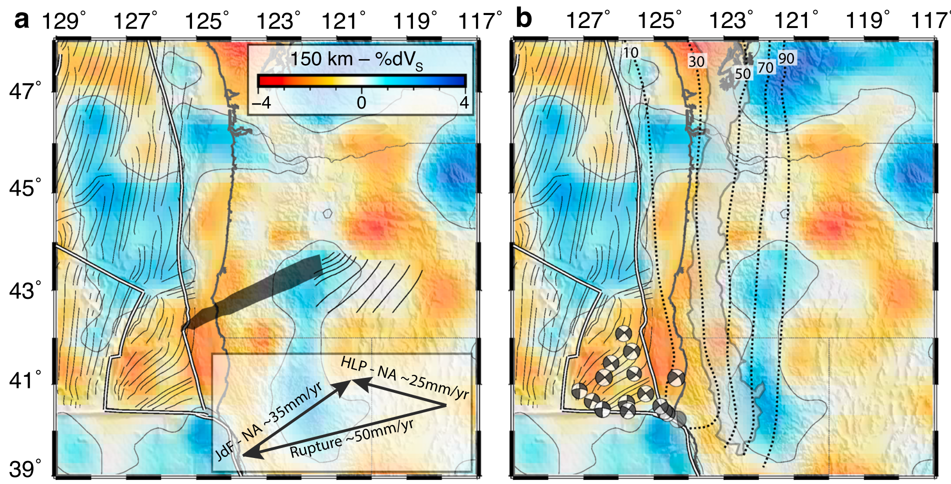

Figure 3. Detailed maps showing the causes and effects of the hole in the Juan de Fuca slab. A slice at 150-km depth through CASC19-S is shown with surface topography in both images. In (a), we focus on the relationship of the hole as seen in tomography with the propagator wake on the Juan de Fuca slab (gray shaded region; Wilson, 2002) and High Lava Plains 1 Ma isochrons (Jordan, 2005). The inset shows the proposed trace of the rupture on the Juan de Fuca slab, calculated by subtracting Juan de Fuca plate motion from the propagation of HLP volcanism, both with respect to North America. In (b), we focus on the resultant deformation of the Juan de Fuca plate. The southern extent of tremor activity (gray shaded region; Wech, 2010) and slab surface contours (dotted lines, labeled in kilometers; McCrory et al., 2012) match the slab extent in CASC19-S, extending well south of the Mendocino Transform. Focal mechanisms are all offshore earthquakes from the GCMT catalogue south of 43°N, with $M_W > 6.3$.

weakness is a possible scenario. The precise depth of the hole is difficult to locate using teleseismic body wave tomography and appears at different depths in different models. Since, however, the resultant volcanism lies to the east of the arc, we can be reasonably confident that the tear is below 100-km depth. We stress that the depth of this deformation will preclude brittle failure—there are no earthquakes clearly associated with the tearing. The slab would instead thin along this weak region, eventually pulling apart (Figure 4).

At first glance, it seems unexpected that the volcanism would rest over the southern edge of the hole, rather than in the middle. Carefully considering the geometry of the slab and propagator wake, and

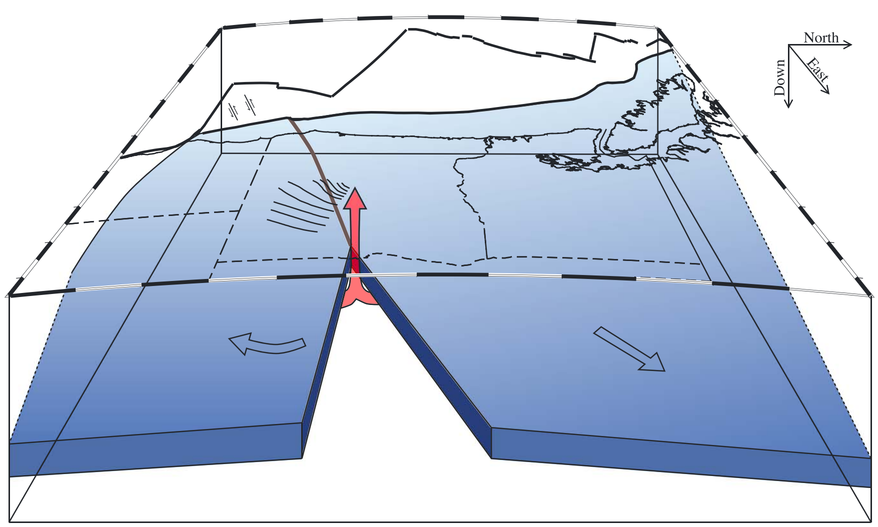

Figure 4. A schematic model that links the slab hole with other physiographic features. The view is from the east, and the Juan de Fuca slab is shown in blue. The propagator wake (bold gray line underneath Oregon) causes a weakness in the slab along which a tear is propagating. The High Lava Plains (contours in Oregon) lie above the southern edge of the slab hole. The Gorda slab rotates clockwise, causing intraplate seismicity in the Gorda region.

10.1029/2019GL083437

uncertainty in the precise shape of the hole as imaged with seismic tomography, helps to explain why the volcanism is over the southern end of the imaged hole. Shear wave splitting measurements (Long et al., 2009) and recent geodynamical modeling (Zhou et al., 2018) indicate the horizontal component of mantle flow is largely east-west, and we thus expect little north-south flow between the tear and the volcanism on the surface. The NE-SW orientation of the propagator wake means that the deeper parts of the feature are situated farther to the north. The southern edge of the hole, then, would extend generally toward the east with depth, while the northern edge of the hole would trend generally to the northeast with depth. Thus the entirety of a hole resulting from this propagator wake will be to the north and east of the shallow tear, and any vertical smearing in the tomographic images will result in low velocities being imaged to the north, but not to the south. We suggest that this is the reason the propagator wake aligns with the southern edge of the imaged hole.

A number of other propagator wakes are mapped in Wilson (2002). Only one of these propagator wakes is larger than the one we show in Figure 3, and it has additionally been associated with increased seismicity (Nedimović et al., 2009). At depth, this propagator wake is not associated with a region of low velocities and thus does not appear to be related to a similar tear in the slab. All of the other (smaller) propagator wakes are well north of our model domain by the time they reach ~100-km depth, and we will not speculate about whether similar tears may be happening elsewhere.

The existence of a propagator wake may not be a necessary condition at all. A tear has developed in the subducting slab in various geodynamic models of the region, both those that use as a starting condition a density field derived from seismic tomography (Zhou, Liu, & Hu, 2018), and those that use only surface constraints to define the boundary conditions (Liu & Stegman, 2011). In particular, these recent geodynamical studies have suggested that both the HLP and the Snake River Plain age-progressive volcanic tracks are a result of hot oceanic asthenosphere intruding into the mantle beneath North America (Zhou, Hu, et al., 2018; Zhou, Liu, & Hu, 2018) and do not explicitly model a hole in the downgoing slab. Thus, while the propagator wake is not necessary for anomalous HLP volcanism in the western United States, it is a specific and striking explanation that connects a structural feature inherited from creation at a mid-ocean ridge with an unusual but robust hole imaged in seismic tomography, and with anomalous volcanism on the overriding North American plate.

4.2. Effects on the Subducting JdF Plate

We have argued, as have other authors, that slabs can tear in the mantle and that this process can generate volcanism above the tear. We also show that the fragmentation of the slab in the mantle may be responsible for deformation within the JdF plate. The disintegration of the slab would allow a clockwise rotation of the southern fragment, which is connected to the Gorda section of the JdF plate. Clockwise rotation of this southern fragment is consistent with the observed southern edge of the subducting slab (Figure 3b). This edge can be seen trending southeastward in a number of data sets, including the extent of nonvolcanic tremor (Wech, 2010), a slab model constrained by microseismicity, and active source seismic studies (McCrory et al., 2012), as well as our own tomographic model. This edge traces back to the Mendocino Transform between the JdF and Pacific plates, which trends east-west. The conjugate fracture zone on the Pacific plate is remarkably straight for more than 1,000 km, also trending east-west. Absent deformation, it would be expected that the southern edge of the JdF slab would maintain the same strike. Wilson (2002) suggests that this is due to the stability of the Mendocino transform despite the rotation of the JdF ridge system. While this “snowplow” effect could generate the observed deformation, it also can be easily explained by clockwise rotation of the southern slab fragment as it moves through the subduction zone and in to the mantle.

Furthermore, the process we propose is consistent with deformation within the Gorda region. This deformation manifests primarily as left-lateral strike-slip faulting on northeast-southwest trending faults. These are found in Gorda crust older than 2 Ma and south of the propagator wake (focal mechanisms in Figure 3b). We suggest these are en echelon faults as a result of clockwise rotation of the Gorda section relative to the Pacific and central JdF plates. Again, while this deformation could be partially explained by the snowplow effect from the rotation of the JdF ridge relative to the Mendocino Transform, the process of slab fragmentation as we describe it here would have the same effect.

4.3. Implications for Subduction Termination

Our connection of nonrigid behavior in the Gorda lithosphere with the fragmentation of the JdF slab at depth suggests that the death of an oceanic plate is a bottom-up process. Instead of subducting normally until the ridge meets the trench, a plate may begin to break apart on the surface as the ridge approaches the trench, driven by fragmentation of a weak slab in the mantle. This should not be surprising, given that, for example, there is significantly more plate surface area that is slab attached to the Gorda section of the JdF plate than there is Gorda lithosphere on the surface. Burkett and Billen (2009) describe numerical models in which slab detachment occurs before ridge subduction; our conceptual model differs from this in two distinct ways: first, the deformation occurs on a preexisting zone of weakness inherited from the formation of the plate, and second, the tear is not occurring laterally, parallel to the trench, but is originating from much deeper in the subducting slab.

If subduction ends before the ridge arrives at the trench, the surviving plate fragment will attach to one of the two plates that is bounding it—in the case of JdF, either the Pacific plate or the North American plate. Older fragments, such as the Magdalena, Guadalupe, and Monterey microplates, are seen in seafloor magnetic data, having been incorporated into the Pacific plate (Nicholson et al., 1994). It has been suggested that these plate fragments have stagnant slabs attached to them, extending into the mantle as deep as 200 km (Wang et al., 2013).

Alternatively, slabs can accrete onto the overriding plate, becoming the building blocks of a new continent. Old terranes, accreted onto North America, may still have visible slab fragments attached to them, such as the Llano and the Cheyenne slabs (Porritt et al., 2014). It is possible that the Gorda, followed by the rest of the JdF, will accrete onto North America in a similar fashion. Regardless of which plate the fragments of the JdF will accrete onto, our analysis suggests that the capture of these oceanic plate fragments is driven by processes in the mantle, which may, in turn, be driven by along-strike variations in the lithospheric structure inherited at the ridge.

5. Conclusions

A holistic analysis of seismic, geologic, petrologic, and marine geophysical data suggests that as the JdF plate nears the end of its life, disintegration of the slab in the mantle drives deformation on the surface. A hole in the subducting JdF slab as seen in seismic tomography is coincident with age-progressive volcanic activity in the HLP, and closely matches a weak zone in the JdF plate, raising the possibility that these three phenomena are related. We suggest that a tear along the weak propagator wake encourages asthenospheric flow through the hole in the slab, generating volcanism in southeastern and central Oregon. The resulting fragmentation of the slab in the mantle affects the stress state on the surface, leading to nonrigid motion in the Gorda section of the JdF plate. Furthermore, comparing with magnetic and seismic studies elsewhere, we suggest that this surficial fragmentation will persist as highly deformed geologic features, and the resulting fragments of the slab, unable to subduct, may accrete onto either the Pacific or the North American lithosphere. If our interpretation is correct, the Gorda section of the JdF plate provides an excellent ongoing example of the processes that govern the demise of a long-lived oceanic plate.

Acknowledgments
We thank M. A. Richards for discussions and comments on the manuscript. Generic Mapping Tools software (Wessel et al., 2013) was used to create the figures. Support for this work was provided by the NSF under Graduate Research Fellowship Program (Grant DGE-1106400 to W. B. H.). The data used in this study are archived by the Data Management Center of the Incorporated Research Institutions for Seismology (http://ds.iris.edu/ds/nodes/dmc/) and by the Northern California Earthquake Data Center (www.ncedc.org; doi:10.7932/NCEDC). The seismic velocity model may be downloaded from the Earth Model Collaboration repository of the Incorporated Research Institutions for Seismology (http://ds.iris.edu/ds/products/emc/).

References

Atwater, T. (1970). Implications of plate tectonics for the Cenozoic tectonic evolution of western North America. *Geological Society of America Bulletin*, *81*(12), 3513. https://doi.org/10.1130/0016-7606(1970)81[3513:IOPTFT]2.0.CO;2

Berk Biryol, C., Beck, S. L., Zandt, G., & Özacar, A. A. (2011). Segmented African lithosphere beneath the Anatolian region inferred from teleseismic *P*-wave tomography. *Geophysical Journal International*, *184*(3), 1037–1057. https://doi.org/10.1111/j.1365-246X.2010.04910.x

Bodmer, M., Toomey, D. R., Hooft, E. E. E., & Schmandt, B. (2018). Buoyant asthenosphere beneath Cascadia influences megathrust segmentation. *Geophysical Research Letters*, *45*, 6954–6962. https://doi.org/10.1029/2018GL078700

Burkett, E. R., & Billen, M. I. (2009). Dynamics and implications of slab detachment due to ridge-trench collision. *Journal of Geophysical Research*, *114*, B12402. https://doi.org/10.1029/2009JB006402

Camp, V. E., & Ross, M. E. (2004). Mantle dynamics and genesis of mafic magmatism in the intermontane Pacific Northwest. *Journal of Geophysical Research*, *109*, B08204. https://doi.org/10.1029/2003JB002838

Canales, J. P., Carbotte, S. M., Nedimović, M. R., & Carton, H. (2017). Dry Juan de Fuca slab revealed by quantification of water entering Cascadia subduction zone. *Nature Geoscience*, *10*(11), 864–870. https://doi.org/10.1038/NGEO3050

Cheng, C., Bodin, T., Tauzin, B., & Allen, R. M. (2017). Cascadia subduction slab heterogeneity revealed by three-dimensional receiver function Kirchhoff migration. *Geophysical Research Letters*, *44*, 694–701. https://doi.org/10.1002/2016GL072142

Dahlen, F. A., Hung, S. H., & Nolet, G. (2000). Fréchet kernels for finite-frequency traveltimes—I. Theory. *Geophysical Journal International*, *141*(1), 157–174. https://doi.org/10.1046/j.1365-246X.2000.00070.x

Ford, M. T., Grunder, A. L., & Duncan, R. A. (2013). Bimodal volcanism of the High Lava Plains and Northwestern Basin and Range of Oregon: Distribution and tectonic implications of age-progressive rhyolites. *Geochemistry, Geophysics, Geosystems*, *14*, 2836–2857. https://doi.org/10.1002/ggge.20175

Graham, D. W., Reid, M. R., Jordan, B. T., Grunder, A. L., Leeman, W. P., & Lupton, J. E. (2009). Mantle source provinces beneath the Northwestern USA delimited by helium isotopes in young basalts. *Journal of Volcanology and Geothermal Research*, *188*(1–3), 128–140. https://doi.org/10.1016/j.jvolgeores.2008.12.004

Han, S., Carbotte, S. M., Canales, J. P., Nedimović, M. R., Carton, H., Gibson, J. C., & Horning, G. W. (2016). Seismic reflection imaging of the Juan de Fuca plate from ridge to trench: New constraints on the distribution of faulting and evolution of the crust prior to subduction. *Journal of Geophysical Research: Solid Earth*, *121*, 1849–1872. https://doi.org/10.1002/2015JB012416

Hawley, W. B., Allen, R. M., & Richards, M. A. (2016). Tomography reveals buoyant asthenosphere accumulating beneath the Juan de Fuca plate. *Science*, *353*(6306), 1406–1408. https://doi.org/10.1126/science.aad8104

Hey, R. (1977). A new class of “pseudofaults” and their bearing on plate tectonics: A propagating rift model. *Earth and Planetary Science Letters*, *37*(2), 321–325. https://doi.org/10.1016/0012-821X(77)90177-7

Horning, G. W., Canales, J. P., Carbotte, S. M., Han, S., Carton, H., Nedimović, M. R., & van Keken, P. E. (2016). A 2-D tomographic model of the Juan de Fuca plate from accretion at axial seamount to subduction at the Cascadia margin from an active source ocean bottom seismometer survey. *Journal of Geophysical Research: Solid Earth*, *121*, 5859–5879. https://doi.org/10.1002/2016JB013228

James, D. E., Fouch, M. J., Carlson, R. W., & Roth, J. B. (2011). Slab fragmentation, edge flow and the origin of the Yellowstone hotspot track. *Earth and Planetary Science Letters*, *311*(1-2), 124–135. https://doi.org/10.1016/j.epsl.2011.09.007

Jordan, B. T. (2005). Age-progressive volcanism of the Oregon High Lava Plains; overview and evaluation of tectonic models. *Special Paper - Geological Society of America*, *388*(30), 503–515. https://doi.org/10.1130/0-8137-2388-4.503

Liu, L., & Stegman, D. R. (2011). Segmentation of the Farallon slab. *Earth and Planetary Science Letters*, *311*(1–2), 1–10. https://doi.org/10.1016/j.epsl.2011.09.027

Liu, L., & Stegman, D. R. (2012). Origin of Columbia River flood basalt controlled by propagating rupture of the Farallon slab. *Nature*, *482*(7385), 386–389. https://doi.org/10.1038/nature10749

Long, M. D., Gao, H., Klaus, A., Wagner, L. S., Fouch, M. J., James, D. E., & Humphreys, E. D. (2009). Shear wave splitting and the pattern of mantle flow beneath eastern Oregon. *Earth and Planetary Science Letters*, *288*(3–4), 359–369. https://doi.org/10.1016/j.epsl.2009.09.039

Long, M. D., Till, C. B., Druken, K. A., Carlson, R. W., Wagner, L. S., Fouch, M. J., et al. (2012). Mantle dynamics beneath the Pacific Northwest and the generation of voluminous back-arc volcanism. *Geochemistry, Geophysics, Geosystems*, *13*, Q0AN01. https://doi.org/10.1029/2012GC004189

McCrory, P. A., Blair, J. L., Waldhauser, F., & Oppenheimer, D. H. (2012). Juan de Fuca slab geometry and its relation to Wadati-Benioff zone seismicity. *Journal of Geophysical Research*, *117*, B09306. https://doi.org/10.1029/2012JB009407

Nedimović, M. R., Bohnenstiehl, D. R., Carbotte, S. M., Pablo Canales, J., & Dziak, R. P. (2009). Faulting and hydration of the Juan de Fuca plate system. *Earth and Planetary Science Letters*, *284*(1-2), 94–102. https://doi.org/10.1016/j.epsl.2009.04.013

Nicholson, C., Sorlien, C. C., Atwater, T., Crowell, J. C., & Luyendyk, B. P. (1994). Microplate capture, rotation of the western Transverse Ranges, and initiation of the San Andreas transform as a low-angle fault system. *Geology*, *22*(6), 491. https://doi.org/10.1130/0091-7613(1994)022<0491:MCROTW>2.3.CO;2

Obayashi, M., Yoshimitsu, J., & Fukao, Y. (2009). Tearing of stagnant slab. *Science*, *324*(5931), 1173–1175. https://doi.org/10.1126/science.1172496

Obrebski, M., Allen, R. M., Xue, M., & Hung, S. H. (2010). Slab-plume interaction beneath the Pacific Northwest. *Geophysical Research Letters*, *37*, L14305. https://doi.org/10.1029/2010GL043489

Pierce, K. L., & Morgan, L. A. (1992). The track of the Yellowstone hot spot: Volcanism, faulting, and uplift. In P. K. Link, M. A. Kuntz, & L. B. Platt (Eds.), *Regional Geology of Eastern Idaho and Western Wyoming: Geological Society of America Memoir* (Vol. 179, pp. 1–53). Geological Sociey of America.

Porritt, R. W., Allen, R. M., & Pollitz, F. F. (2014). Seismic imaging east of the Rocky Mountains with USArray. *Earth and Planetary Science Letters*, *402*(C), 16–25. https://doi.org/10.1016/j.epsl.2013.10.034

Portner, D. E., Beck, S. L., Zandt, G., & Scire, A. (2017). The nature of subslab slow velocity anomalies beneath South America. *Geophysical Research Letters*, *44*, 4747–4755. https://doi.org/10.1002/2017GL073106

Rosenbaum, G., Gasparon, M., Lucente, F. P., Peccerillo, A., & Miller, M. S. (2008). Kinematics of slab tear faults during subduction segmentation and implications for Italian magmatism. *Tectonics*, *27*, TC2008. https://doi.org/10.1029/2007TC002143

Roth, J. B., Fouch, M. J., James, D. E., & Carlson, R. W. (2008). Three-dimensional seismic velocity structure of the northwestern United States. *Geophysical Research Letters*, *35*, L15304. https://doi.org/10.1029/2008GL034669

Schmandt, B., & Humphreys, E. D. (2010). Complex subduction and small-scale convection revealed by body-wave tomography of the western United States upper mantle. *Earth and Planetary Science Letters*, *297*(3–4), 435–445. https://doi.org/10.1016/j.epsl.2010.06.047

Till, C. B., Grove, T. L., Carlson, R. W., Donnelly-Nolan, J. M., Fouch, M. J., Wagner, L. S., & Hart, W. K. (2013). Depths and temperatures of <10.5 Ma mantle melting and the lithosphere-asthenosphere boundary below southern Oregon and northern California. *Geochemistry, Geophysics, Geosystems*, *14*, 864–879. https://doi.org/10.1002/ggge.20070

Toomey, D., Allen, R., Barclay, A., Bell, S., Bromirski, P., Carlson, R., et al. (2014). The Cascadia initiative: A sea change in seismological studies of subduction zones. *Oceanography*, *27*(2), 138–150. https://doi.org/10.5670/oceanog.2014.49

Wang, Y., Forsyth, D. W., Rau, C. J., Carriero, N., Schmandt, B., Gaherty, J. B., & Savage, B. (2013). Fossil slabs attached to unsubducted fragments of the Farallon plate. *Proceedings of the National Academy of Sciences*, *110*(14), 5342–5346. https://doi.org/10.1073/pnas.1214880110

Wech, A. G. (2010). Interactive tremor monitoring. *Seismological Research Letters*, *81*(4), 664–669. https://doi.org/10.1785/gssrl.81.4.664

Wessel, P., Smith, W. H. F., Scharroo, R., Luis, J., & Wobbe, F. (2013). Generic Mapping Tools: Improved version released. *Eos, Transactions American Geophysical Union*, *94*(45), 409–410. https://doi.org/10.1002/2013EO450001

Wilson, D. S. (1989). Deformation of the so-called Gorda Plate. *Journal of Geophysical Research*, *94*(B3), 3065–3075. https://doi.org/10.1029/JB094iB03p03065

Wilson, D. S. (1990). Kinematics of overlapping rift propagation with cyclic rift failure. *Earth and Planetary Science Letters*, *96*(3-4), 384–392. https://doi.org/10.1016/0012-821X(90)90014-O

Wilson, D. S. (1993). Confidence intervals for motion and deformation of the Juan de Fuca Plate. *Journal of Geophysical Research*, *98*(B9), 16,053. https://doi.org/10.1029/93JB01227

Wilson, D. S. (2002). The Juan de Fuca plate and slab: Isochron structure and Cenozoic plate motions. In E. S. Kirby, K. Wang, & S. Dunlop (Eds.), *The Cascadia Subdunction Zone and Related Subduction Systems—Seismic Structure, Intraslab Earthquakes and Processes, and Earthquake Hazards: U.S. Geological Survey Open-File Report 02-328* (182 pp.). Menlo Park, CA.

Zhou, Q., Hu, J., Liu, L., Chaparro, T., Stegman, D. R., & Faccenda, M. (2018). Western U.S. seismic anisotropy revealing complex mantle dynamics. *Earth and Planetary Science Letters*, *500*, 156–167. https://doi.org/10.1016/j.epsl.2018.08.015

Zhou, Q., Liu, L., & Hu, J. (2018). Western US volcanism due to intruding oceanic mantle driven by ancient Farallon slabs. *Nature Geoscience*, *11*(1), 70–76. https://doi.org/10.1038/s41561-017-0035-y